



# Effect of linkage design of an elbow implant on micro-motion: a finite element analysis

Milad Heidari<sup>1\*</sup>, Pooyan Rahmanivahid<sup>1</sup>

<sup>1</sup>Mechanical Engineering and Vehicle Technology Department, Global College of Engineering and Technology (GCET), P.O. Box 2546 CPO Ruwi 112, Muscat, Sultanate of Oman

\*Corresponding author E-mail: [milad@gcet.edu.om](mailto:milad@gcet.edu.om)

## Abstract

The major reason for total elbow arthroplasty failure is loosening. Loosening is the outcome of a detrimental mechanical incident, which causes the failure of the bond between the bone bed and implant. The shape of the linkage of an elbow implant has a considerable role to transfer a portion of the load to the cement-bone and cement-implant interfaces. Therefore, in this study, the linkage of an elbow implant was modified to reduce loosening using finite element analyses. Elbow bone was constructed using image processing software. Linkage components were modeled using modeling computer-aided design software. Material properties and boundary conditions were applied. The stress distribution and micro-motion were obtained in linkage component and cement-implant-bone interfaces respectively. Based on our results, sub-design 3B proved less interface micro-motion compared to others. Our study showed that modification of a linkage reduces the micro-motion transferred to bone-cement and cement-implant interfaces. A reduction of micro-motion, through linkage modification, may improve the clinical outcomes.

**Keywords:** Elbow Implant; Finite Element Analysis; Loosening; Micro-Motion; Stress Distribution.

## 1. Introduction

Total elbow arthroplasty (TEA) is one of the most reliable alternative treatments for restoring the function of failed elbows [1 - 4]. There are several elbow implant designs, which may significantly differ from each other. Although an increased survival rate of elbow implants has been reported in the presence of modern linked implants, loosening has remained a major concern [5, 6]. Loosening is the outcome of a detrimental mechanical incident, which causes the failure of the bond between the bone bed and implant. The shape of elbow implant linkage has a considerable role to transfer a portion of the load to the distal humerus, cement-bone, and cement-implant interfaces. This is because of the amounts of the transferred load from the implant stem to the bone which can be raised by linkage design [7 - 9].

In attempts to find more knowledge of the biomechanics of the elbow, scientists have modified the implant design and the long-term results of TEA have been distinctly enhanced. A simple hinge joint was the basis of most of the original designs; consequently, the failure by loosening was the result of the intrinsic complete constraint of the articulation. Two designs are utilized based on modern elbow implants: unlinked or linked hinge [10 - 13]. Various designs of implants may significantly differ from each other. These diversities in different designs are about the carrying angle consideration and how this angle is combined through either the humeral or ulnar implant. The hinged principle is the basis of linked implants. How the humeral and ulnar components linked at the surgery time, (prevents dislocation), is the feature by this category. Connection parts are the pins or snap-fit bushings. These parts provide a semi-constrained hinged structure that allows a little laxity in different directions (medial, lateral, and rotational planes). This structure has been considered as an accurate simulation of a loose hinge in normal elbow kinematics [14 - 16].

More reliable long-term fixation was the result of semi-constrained implants. This is due to less stress transmission within the implant interfaces and some supplementary improvements. The linked implants receive higher forces than unlinked implants and consequently loosening is encouraged [7], [15], [17]. There are four linked implants systems available called the Coonrad-Morrey (Zimmer, Warsaw, IN), the Discovery (Biomet, Warsaw, IN), the Latitude (Tornier, Stafford, TX), and the Solar (Stryker, Mahwah, NJ) implant systems. While here are some similar features in the designs of these implants, some features of these designs differ from each other.

The major reason for TEA failure is loosening. Loosening manifests itself as micro-motion (relative motion between the bone, cement, and implant). The survival rate of TEA has been improved by modern linked implants. However, a problem has remained unsolved in loosening. There is a need to develop and modify implant features to attain improved results. The Success of elbow implants depends on the way mechanical factors are transferred to the surrounding bone and interfaces.

The modifications of the existing linked implant should be established by improving different parameters such as linkage to contribute to the longevity and functionality of the replacement [15], [18 - 21]. Although there are a large number of studies on design parameters of elbow implants, studies on the state of micro-motion due to modification of linkage are limited according to the author's knowledge. Therefore, TEA suffers from a lack of computational study in the modification of linkages to decrease loosening. Hence, this paper aims

to evaluate the impact linkage design on micro-motion in the cement-bone-implant interfaces to initiate implant loosening. The present study modified the linkage of an elbow implant to reduce loosening before clinical usages using finite element analyses (FEA).

## 2. Materials and methods

Mimics software (Ver.10, Materialise NV., Belgium) was used to construct elbow bone (humerus). The elbow bone was achieved from a 3D construction of CT data set from a healthy elbow of a male with a resolution of 0.477mm and a slice thickness of 0.7mm (Figure 1). Then, the constructed elbow bone was imported into SolidWorks software (DassaultSystemes SolidWorks Corp, USA) to model and analyze of implant linkage.

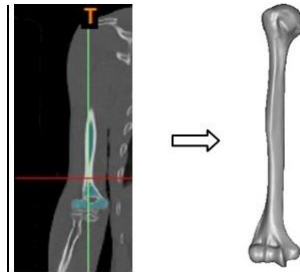


**Fig. 1:** Constructed Bone from CT Scan Data.

A few linked elbow implant systems are commercially available, including cylindrical (CY), hourglass (HG) and concave cylinder (CC). Each design features an axle as the articular geometry of the humeral component which articulates against a polyethylene bearing of the ulnar component [22]. The intercondylar region of the humerus bone was important to modify the curve of linkage. A humeral component was modified using previous designs. The curve obtained from the intercondylar of the elbow (Figure 2). A humeral axle of bearing surface was modified assisting the curve of trochlea. The diameter of the humeral axle went smaller from the trochlea to capitulum. Polyethylene bushing was developed to articulate against axle of the humeral component. This was inserted inside the hole of the ulnar component (Figure 4).

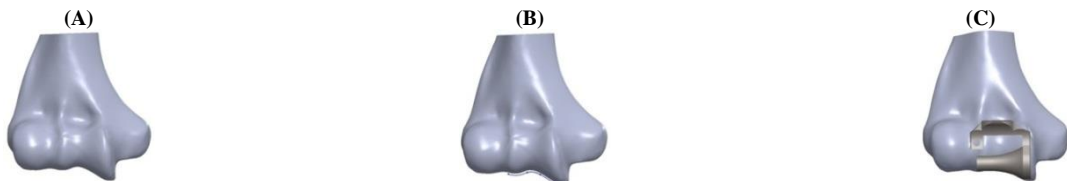


**Fig. 2:** (A) Front View of Distal Bone (B) Surveying Curve of Trochlea (C) Matching Modified Humeral Bearing Axle Considering Trochlea Curve.

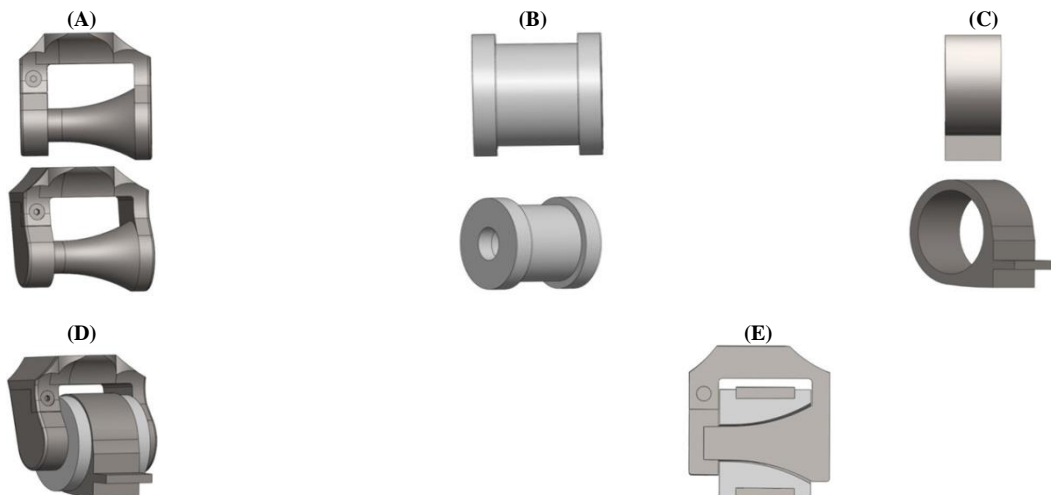


**Fig. 3:** Modified Linkage Mechanism (A) Humeral Component (B) Polyethylene Bushing (C) Ulnar Component (D) Assembly (E) Cross-Section.

Furthermore, several polyethylene sizes and shapes were modeled (Figure 4). Based on each polyethylene shape and size, related proximal humeral/ulnar components were modeled with various sizes and shapes. Three cases were defined for each modeled polyethylene and proximal humeral/ulnar components.

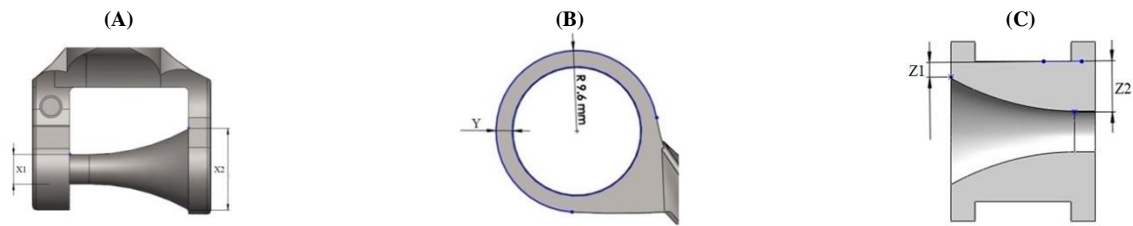


**Fig. 4:**Modified Linkage (A) Humeral Yoke (B) Proximal Ulnar Component Thickness (C) Polyethylene Bushing.

In case 1 (Table 1), the diameter of modified humeral yoke articulates with the medial and lateral aspect of the proximal ulnar. This diameter was considered 4 mm in the smallest side and 11 mm in the largest one. According to the pointed diameter, various polyethylene thicknesses and proximal ulnar bearing surfaces were determined. In case 2, the diameter of the modified humeral yoke was considered 5 mm in the smallest side and 12 mm in the largest side. According to the pointed diameter, various polyethylene thicknesses and proximal ulnar bearing surfaces were determined. In case 3, the diameter of the modified humeral yoke was considered 6 mm in the smallest side and 13 mm in the largest one. According to the pointed diameter, various polyethylene thicknesses and proximal ulnar bearing surfaces were determined. Critical dimensions for controlling the conformity were parameterized. These dimensions allow the conformity characteristics of modeled linkage to be easily adjusted (Figure 5). These parameters included the frontal radii of curvature for the humeral (RH) and ulnar (RU) component. For this linkage 4° conformity was used as  $R_H - R_U = 2.5\text{mm}$  [22].

**Table 1:**Modified Linkage in Case 1, 2, and 3

Parameters	Case 1A	Case 1B	Case 1C	Case 2A	Case 2B	Case 2C	Case 3A	Case 3B
X1(mm)	4	4	4	5	5	5	6	6
X2(mm)	11	11	11	12	12	12	13	13
Z1(mm)	2	1.5	1	1.5	2	2.5	1	1.5
Z2(mm)	5.7	5.2	4.7	5.2	5.7	6.2	4.7	5.2
Y(mm)	1.5	2	2.5	1.5	2	1.5		

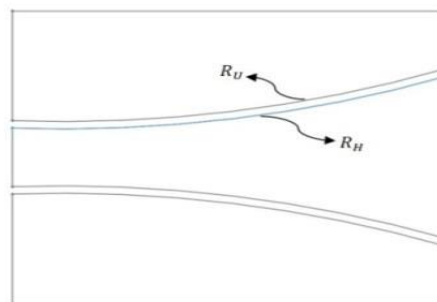


**Fig. 5:**Parametric Geometry for Adjusting Conformity.

To study the stress in linkage components, a perfect bond was assumed at the ulnar component and polyethylene. Surface-to-surface contact was considered for humeral component and polyethylene bushing. Friction was modeled with a coefficient of 0.04 [2], [23 - 26]. A 20 N compression load was applied at the tip of an ulnar component (Figure 6). Zero-displacement was applied at the humeral component



**Fig. 6:**Modified Linkage (A) Boundary Condition (B) Applied Force.

To study micro-motion in cement- implant and cement-bone interfaces, the modified linkage was attached to the humeral component stem (Implant stem) and inserted in the bone. Figure 7 illustrates the insertion of the humeral component (linkage + stem) into the bone. The proximal end of the model was fixed. A 20 N compression load was applied at the tip of an ulnar component. Conventional cemented fixation was the basis of modeling therefore, they had smooth surfaces. The thickness of the cement was 1.5 mm. Furthermore, a mesh convergence was carried out and a mesh size of 1 mm was chosen for this study.

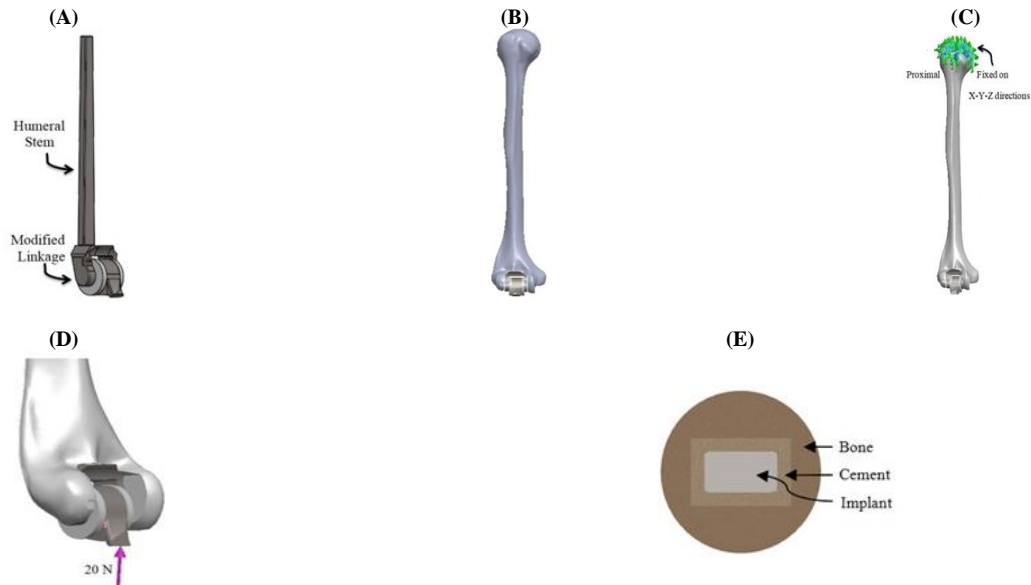


**Fig. 7:** (A) Linkage Attached to Humeral Stem (B) Placement of Implant Into the Bone (C) Boundary Condition (D) Applied Force (E) Cement Used Around Stem.

Table 2 contains the material properties of the implant and bone. Homogeneous, isotropic and linear elastic materials were assumed. There was an assumption of a perfect bond at the interfaces between bone-cement and cement-implant [27, 28, 29, 30, 31, 32].

**Table 2:** Mechanical Properties of Materials

Material	Elastic module (GPa)	Poisson ratio
Humeral/Ulnar component (Titanium)	110	0.3
Bone	20	0.3
Cement	2.28	0.3
Polyethylene	1	0.3

The FEA method presents the amount of sliding which happens at the interface through subtracting displacement of outer cement surface from the bone surface and also the displacements at cement surface from the outer surface of the stem. Hence, in this study, micro-motion was defined as the relative displacement of a specific component within a mechanical system. Calculating implant micro-motion by subtracting displacement values for the bone and implant confirmed the general trends observed by comparing the different finite element models [86]. Thus, the extent of the micro-motion of the model was estimated using the difference in average displacement between the bone, cement, and prosthesis.

### 3. Results and discussion

The Von-Mises stress distributions were obtained throughout the polyethylene bushing and humeral components of each linkage under 20N of axial load. As seen in Figures 8, 9 and 10 a similar pattern of stress distribution was seen for polyethylene bushing in all three cases (1, 2, 3). The most stress was seen where polyethylene bushing contacted the narrower part of the humeral axle, while no stresses were seen where polyethylene bushing contacted the wider part of the humeral axle.

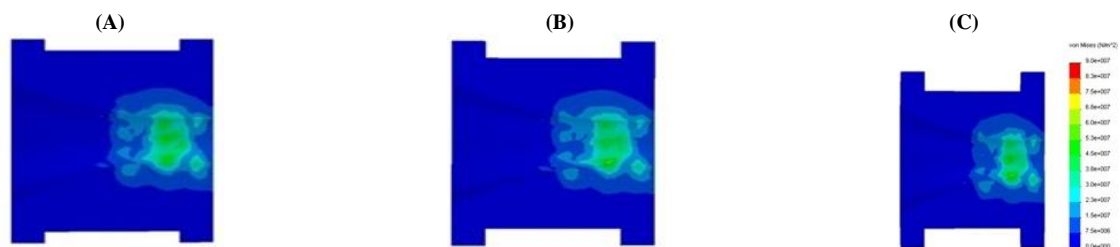


**Fig. 8:** Von Mises Stress Plot for Different Polyethylene Bushings in Case 1 (A) Case 1A (B) Case 1B (C) Case 1C.

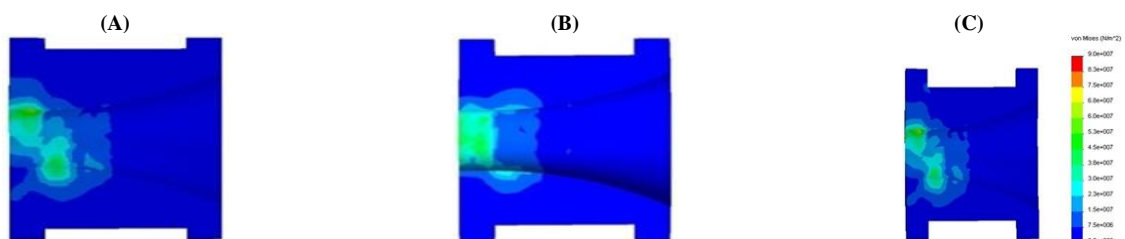


**Fig. 9:** Von Mises Stress Plot for Different Polyethylene Bushing in Case 2 (A) Case 2A (B) Case 2B (C) Case 2.



Fig. 10: Von Mises Stress Plot for Different Polyethylene Bushing in Case 3 (A) Case 3A (B) Case 3B.

Figures 11, 12 and 13 show stress for the humeral axle in each case. Stress distributions were reduced moving from a smaller diameter to a bigger diameter of the humeral axle. The smaller diameter experienced the most stress, while no stress was seen in a bigger diameter of the humeral axle in all cases. Fewer regions of the humeral axle were undergone stress in case 3 in comparison with cases 1 and 2.

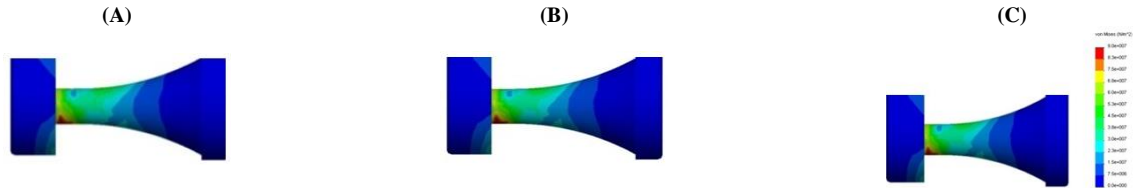


Fig. 11: Von Mises Stress Plot for Modified Humeral Component Related to Different Polyethylene Bushing Sizes in Case 1 (A) Case 1A (B) Case 1B (C) Case 1C.

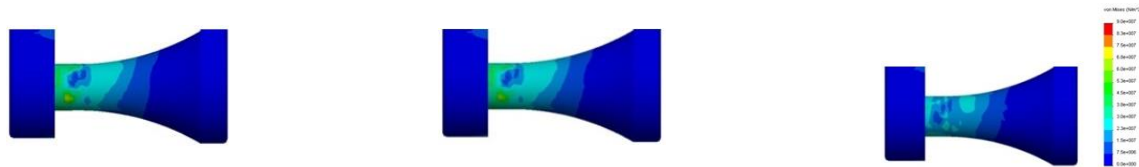


Fig. 12: Von Mises Stress Plot for Modified Humeral Component Related to Different Polyethylene Bushing Sizes in Case 2 (A) Case 2A (B) Case 2B (C) Case 2C.



Fig. 13: Von Mises Stress Plot for Modified Humeral Component Related to Different Polyethylene Bushing Sizes in Case 3 (A) Case 3A (B) Case 3B.

Based on the results, less stress was seen for subsections of C, C, and B for cases 1, 2 and 3 respectively. Therefore, micro-motion transferred through these linkages to bone-cement-implant interfaces of humerus bone was obtained. Micro-motion transferred to the bone-cement interface related to each linkage is shown in Fig. 14 (a). There was a decreased trend in micro-motion from Case 1C to Case 3B. Case 1C showed micro-motion at 48  $\mu\text{m}$ , while Case 2C expressed 36  $\mu\text{m}$ . Case 3B transmitted the least micro-motion at 32  $\mu\text{m}$  to the bone-cement interface. Fig. 14 (b) shows the micro-motion in the cement-implant interface for the same linkages. A similar trend was seen. The highest micro-motion was observed for Case 1C at 45  $\mu\text{m}$ , while the lowest value was seen for Case 3B at only 34  $\mu\text{m}$ . Case 2C transferred micro-motion at 31  $\mu\text{m}$  to the cement-implant interface.

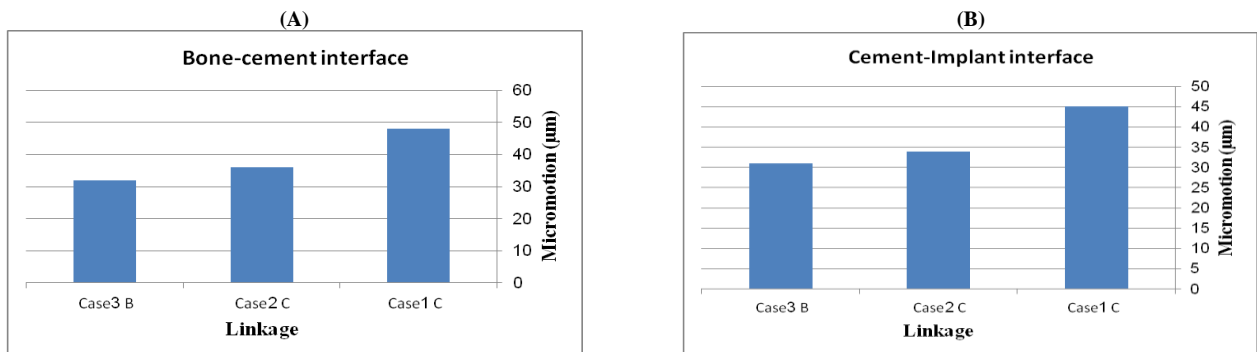


Fig. 14: Micro-Motion for Three Modified Linkage (A) Bone-Cement Interface (B) Cement-Implant Interface.

The stress on polyethylene components of other joint replacement systems has been investigated using FEA [33 - 35]. The usefulness of FEA has been proved for the study of implant component stress. Moreover, there is an ability of articular contact parameters determination, which is difficult to measure. To overcome reducing mechanical factors, a linkage was modified considering available commercial

implants and the shape of the distal humerus. The humeral axle was made with the curve of the intercondylar of the elbow. Different thicknesses for polyethylene bushing and as well as various diameters for the axle of the humeral component were considered.

According to the results, sub-design 3B proved less interface micro-motion compared to others. But how this issue is translated into less loosening? Loosening is hypothesized to be the result of a harmful combination of mechanical and biological events, which causes the destruction of the bond between implant and bone bed. Previously, it has been shown that implants with the higher loosening rate have increasing displacement; whereas the implants with the lower loosening rate have decreasing displacement in interfaces. Micro-motion at the bone-cement-implant interfaces predominantly has to be considered as an engineering issue, which should primarily be addressed by the implant designers. Consequently, less micro-motion gives less loosening.

Commercially there are three types of design concepts of linked, including CY, HG, and CC, and each design consisted of a linked humeral and ulnar component to accommodate unrestricted flexion-extension motions and rotations. Our modified linkage consisted of all similar components. Nevertheless, the axle of the humeral component and polyethylene bearing of the ulnar component shape were modified differently. The dimensions for the modified linkage were selected to be reflective of commercially available linked TEA of that specific design concept. According to previous studies, 4° conformity level was chosen to include the Varus-valgus (VV) laxity.

The threshold value of radiolucency has been studied in a few clinical studies. This threshold is believed to be an indicator of the loosening of the linked elbow implant. A study showed 2 mm radiolucency or any type of radiolucency around the implant stems as a sign of loosening [36]. Kleinlugtenbelt et al. showed radiolucent lines around stem >1 mm as the entire loosening [37]. Gilot et al. found loosening of the humeral stem with radiolucent line 2 mm [38]. Therefore, it can be concluded that the threshold of radiolucency lines to predict loosening of elbow implant is the presence of radiolucent lines between 1 mm to 2 mm around stems.

As mentioned, modified linkage with sub-designed 3B transferred less micro-motion to distal humeral stem than other models. The linkage can greatly affect transmitting micro-motion of the distal humeral stem. The higher micro-motion causes the growth of fibrous membrane the bone-implant interface, making the implant unstable [23]. Furthermore, increased micro-motion results in higher movement between surfaces, in which widens the boundaries in bone-cement-implant interfaces and implant component migration. This migration clinically is shown as radiolucency around the stem. If this radiolucency exceeds more than 2 mm, loosening is likely to occur. Therefore, less micro-motion transferred by sub-design 3B to bone-cement-implant interfaces can finally result in less loosening.

Willing et al. investigated the effect of three linkage design on stress and loosening using FEA [22]. Stress distributions of three linked elbow design concepts, including CY, HG, and CC were investigated. The results suggested that the bearing of the CY design increases Von Mises stresses. The CC design also provided low stresses which may mean less stress transfer to interfaces and finally less loosening. Similarly, our results proved the effectiveness of a different design on stress distribution and finally less micro-motion transferred to the interfaces.

One important distinction between finite element predictions and experimental study of micro-motion is where the measurement of relative motion is made. Experimental micro-motion normally contains displacement transducers mounted on the outer cortex of the bone. On the other hand, an FEA micro-motion study calculates how much sliding happens at the interface by subtracting the displacements at the outer surface of the stem from the displacements of the cement surface, and the outer surface of the cement from the displacements of the bone surface in contact with the cement. The outcomes are normally compared with each other, and those with lesser micro-motion are assumed to be better than those with higher micro-motion. The above micro-motion outcomes were proper for the comparison of micro-motion between implants.

Several limitations were observed in the current study. Only a transverse loading was used to analyze the study and considering complex loading such as axial and torsion may present more reliable results. Using elbow with different sizes may support the contribution of the optimized implant stronger. Furthermore, considering cancellous bone in the analysis may deliver more accurate results. It is hoped that future studies may be able to accommodate these deficiencies which may or may not play an important role in the more accurate design of linkage. A wide range of recommendations can be stated for future extensions of the introduced approach in this study. Using the same approach, remodeling of the distal humerus can be investigated due to the modification of linkage. In addition to this, the effect of implant materials along with the modification of linkage may be interesting research for the future. Furthermore, future work can concern the analysis of introduced linkage on the wear of polyethylene.

## 4. Conclusion

In this study, a 3D model of elbow bone was constructed using Mimics software. Humeral and ulnar components of linkage were modeled and analyzed using Solidworks software. Several polyethylene sizes and shapes were modeled to obtain micro-motion in cement-implant-bone interfaces and stress in linkage components using FEA. Our study showed that how modification of a linkage affects micro-motion transferred to bone-cement-implant interfaces. A reduction of micro-motion, through design modifications, may improve the clinical outcomes for both humeral and ulnar components. Dimensions for modified linkage were selected to be reflective of commercially available linked TEA.

## Acknowledgement

We acknowledge Global College of Engineering and Technology of Oman for supporting the study

## References

- [1] McDonald CP, Peters TM, Johnson JA & King GJW (2011), "Stem Abutment Affects Alignment of the Humeral Component in Computer-assisted Elbow Arthroplasty", *J Shoulder Elbow Surg.*, Vol. 20, pp.891-898. <https://doi.org/10.1016/j.jse.2010.12.012>.
- [2] Heidari M, Harun MN & Syahrom A (2014), "Influence of polyethylene thickness on axis pin in linked elbow implant", *Advanced Materials Research*, Vol.845, pp.194-198. <https://doi.org/10.4028/www.scientific.net/AMR.845.194>.
- [3] An KN (2005), "Kinematics and Constraint of Total Elbow Arthroplasty", *J. Shoulder Elbow Surg.*, Vol. 14, pp.168-173. <https://doi.org/10.1016/j.jse.2004.09.035>.
- [4] Heidari M, Harun MN, Kadir MRA., Kashani J & Syahrom A (2013), "Effect of humeral stem shape on displacement in elbow implant", *Applied Mechanics and Materials*, Vol. 393, pp.467-471. <https://doi.org/10.4028/www.scientific.net/AMM.393.467>.
- [5] Lee BP, Adams RA & Morrey BF (2005), "Polyethylene Wear After Total Elbow Arthroplasty", *J. Bone Joint Surg. Am*, Vol. 87, pp.1080-1087. <https://doi.org/10.2106/JBJS.D.02163>.



- [6] Wright, TW & Hastings H (2005), "Total Elbow Arthroplasty Failure due to Overuse, C-ring Failure, and/or Bushing Wear", *J. Shoulder Elbow Surg.*, Vol. 14, pp.65-72. <https://doi.org/10.1016/j.jse.2004.04.015>.
- [7] Chafik D, O'Driscoll S, King GW & Yamaguchi K (2010), "Total Elbow Arthroplasty-Convertible", *Oper. Tech. Orthop.*, Vol. 20, pp.58-67. <https://doi.org/10.1053/j.oto.2009.10.002>.
- [8] Antuna S & Vallina V (2006), "Elbow Arthroplasty: Design, Indications and Results", *Rev. Ortop. Traumatol.*, Vol. 50, pp.55-67. [https://doi.org/10.1016/S0482-5985\(06\)74934-3](https://doi.org/10.1016/S0482-5985(06)74934-3).
- [9] Austman RL, and Beaton BJB, Quenneville CE, King, GJW, Gordon KD & Dunning CE (2007), "The Effect of Distal Ulnar Implant Stem Material and Length on Bone Strains", *J. Hand Surg.*, Vol. 32, pp. 848-854. <https://doi.org/10.1016/j.jhsa.2007.03.013>.
- [10] Heidari M, Rafiq MAK, Fallahiazoodar A & Alizadeh M (2011), "Stress distribution analysis on semi constrained elbow prosthesis during flexion and extension motion", *IFMBE Proceedings*, Vol. 35, pp.215-218. [https://doi.org/10.1007/978-3-642-21729-6\\_57](https://doi.org/10.1007/978-3-642-21729-6_57).
- [11] Heidari M, Rafiq MAK, Kashani J, Fallahiazoodar A, Alizadeh M, Robson N, Kamarul T & Harun MN (2013), "Influences of rheumatoid arthritis on elbow: A finite element analysis", *J. Advanced Science Letters*, Vol. 19, No. 11, pp.3219-3222. <https://doi.org/10.1166/asl.2013.5127>.
- [12] Trigg SD (2006), "Total Elbow Arthroplasty: Current Concepts", *Northeast Florida Med.*, Vol. 57, No. 3, pp.37-40
- [13] An KN (2005), "Kinematics and Constraint of Total Elbow Arthroplasty", *J. Shoulder Elbow Surg.*, Vol. 14, pp.168-173, 2005. <https://doi.org/10.1016/j.jse.2004.09.035>.
- [14] An K & Morrey BF, *Biomechanics of the Elbow, The Elbow and its Disorders*, WBSaunders: Philadelphia (2000).
- [15] Sotelo JS (2010), "Total Elbow Arthroplasty", *J. Open Orthop.*, Vol. 5, pp.115-123. <https://doi.org/10.2174/1874325001105010115>.
- [16] Heidari M., Harun MN, Rafiq MAK, Kashani J & Syahrom A (2013), "Effect of humeral stem shape on displacement in elbow implant", *Applied Mechanics and Materials*, Vol. 393, pp.467-471. <https://doi.org/10.4028/www.scientific.net/AMM.393.467>.
- [17] Lee DH (2011), Linked Total Elbow Arthroplasty. *Hand Clin.*, vol. 27, pp. 199-213. <https://doi.org/10.1016/j.hcl.2011.01.004>.
- [18] Cesar M, Roussanne Y, Bonnel F & Canovas F (2007), "GSB III Total Elbow Replacement in Rheumatoid Arthritis", *J. Bone Joint Surg. Br.*, Vol. 89, pp.330-334. <https://doi.org/10.1302/0301-620X.89B3.18488>.
- [19] Cheung EV & O'Driscoll SW (2007), "Total Elbow Prosthesis Loosening Caused by Ulnar Component Pistoning", *J Bone Joint Surg Am.* Vol. 89, pp.1269-74. <https://doi.org/10.2106/00004623-200706000-00015>.
- [20] Hildebrand KA, Patterson SD, Regan WD, MacDermid JC & King GJ (2000), "Functional Outcome of Semiconstrained Total Elbow Arthroplasty", *J. Bone Joint Surg. Am.*, Vol. 82, pp. 1379-1386. <https://doi.org/10.2106/00004623-200010000-00003>.
- [21] Heidari M, Rafiq MAK, Fallahiazoodar A, Harun MN, Alizadeh M & Kashani J (2012), "Biomechanical assessment of unconstrained elbow prosthesis after total elbow replacement: A finite element analysis", *Applied Mechanics and Materials*, Vol. 234, pp.7-10. <https://doi.org/10.4028/www.scientific.net/AMM.234.7>.
- [22] Willing R, King GJW & Johnson JA (2012), "The Effect of Implant Design of Linked Total Elbow Arthroplasty on Stability and Stress: a Finite Element Analysis", *Computer Meth. Biomech. Biomed. Eng.*, pp.1-8.
- [23] Stokdijk M, Veeger HEJ, de Boera YA & Kozing PM (1999), "Determination of the Optimal Elbow Axis for Evaluation of Placement of Prostheses", *Clin. Biomechan.*, Vol. 4, pp. 177-184. [https://doi.org/10.1016/S0268-0033\(98\)00057-6](https://doi.org/10.1016/S0268-0033(98)00057-6).
- [24] Kedgley AE, Lang P & Dunning CE (2007), "The Effect of Cross-Sectional Stem Shape on the Torsional Stability of Cemented Implant Components", *J. Biomech. Eng.*, Vol. 129, pp.310-314. <https://doi.org/10.1115/1.2720907>.
- [25] Godest AC, Beaugonin M, Haug E, Taylor M & Gregson PJ (2002), "Simulation of a Knee Joint Replacement During a Gait Cycle Using Explicit Finite Element Analysis", *J. Biomech.*, Vol. 35, No. 2, pp.267-275. [https://doi.org/10.1016/S0021-9290\(01\)00179-8](https://doi.org/10.1016/S0021-9290(01)00179-8).
- [26] Halloran JP, Petrella AJ & Rullkoetter PJ (2005), "Explicit Finite Element Modelling of Total Knee Replacement Mechanics", *J. Biomech.*, Vol. 38, No.2, pp. 323-331. <https://doi.org/10.1016/j.jbiomech.2004.02.046>.
- [27] Goel VK, Lee II-K & Blair WF (1989), "Effect of the Coonrad Elbow Prosthesis on Stresses in the Humerus", *J. Clin. Biomech.*, Vol. 4, pp.11-16. [https://doi.org/10.1016/0268-0033\(89\)90062-4](https://doi.org/10.1016/0268-0033(89)90062-4).
- [28] Completo A, Pereira J, Fonseca F, Ramos A, Relvas C & Simões J (2011), "Biomechanical Analysis of Total Elbow Replacement with Unlinked iBP Prosthesis: An in Vitro and Finite Element Analysis", *Clin. Biomechan.*, Vol. 26, pp.990-997. <https://doi.org/10.1016/j.clinbiomech.2011.06.008>.
- [29] Amarasinghe RS, Rupasinghe RAM, Anurathan P & Herath SR (2011), "Effects of Geometry of the Interamedullary Stem of the Ulna Component of Hinged Elbow Joint Prostheses on the Bone and Implant Bending Stress", *J. Mech. Med.Biol.*, Vol. 11, No.5, pp.1271-1293. <https://doi.org/10.1142/S0219519411004228>.
- [30] Prasad N & Dent C (2010), "Outcome of Total Elbow Replacement for Rheumatoid Arthritis: Single Surgeon's Series with Souter-Strathclyde and Coonrad-Morrey Prosthesis", *J. Shoulder Elbow Surg.*, Vol. 19, pp.376-683. <https://doi.org/10.1016/j.jse.2009.09.016>.
- [31] Closkey RF, Goode JR, Kirschenbaum D & Cody RP (2000), "The Role of the Coronoid Process in Elbow Stability. A Biomechanical Analysis of Axial Loading", *J. Bone Joint Surg. Am.*, Vol. 82, pp.1749-1753. <https://doi.org/10.2106/00004623-200012000-00009>.
- [32] Yongpravat C, Kim HM, Gardner TR, Bigliani LU, Levine WN & Ahmad GS (2013), "Glenoid Implant Orientation and Cement Failure in Total Shoulder Arthroplasty: A Finite Element Analysis", *J. Shoulder Elbow Surg.*, Vol. 22, pp.940-947. <https://doi.org/10.1016/j.jse.2012.09.007>.
- [33] Godest, AC, Beaugonin M, Haug E, Taylor M & Gregson PJ (2002), "Simulation of a Knee Joint Replacement During a Gait Cycle Using Explicit Finite Element Analysis", *J. Biomech.*, Vol. 35, No. 2, pp.267-275. [https://doi.org/10.1016/S0021-9290\(01\)00179-8](https://doi.org/10.1016/S0021-9290(01)00179-8).
- [34] Willing R & Kim IY (2009), "A Holistic Numerical Model to Predict Strain Hardening and Damage of UHMWPE Under Multiple Total Knee Replacement Kinematics and Experimental Validation", *J. Biomech.* Vol. 42, No.15, pp.2520-2527. <https://doi.org/10.1016/j.jbiomech.2009.07.008>.
- [35] Matsoukas G, Willing R & Kim IY (2009), "Total Hip Wear Assessment: A Comparison Between Computational and in Vitro Wear Assessment Techniques Using ISO Loading and Kinematics", *J. Biomech. Eng.*, Vol. 31, No.4, <https://doi.org/10.1115/1.3049477>.
- [36] Sneftrup SB, Jensen SL, Johannsen HV & Søjbjerg JO (2006), "Revision of Failed Total Elbow Arthroplasty with Use of a Linked Implant", *J. Bone & Joint*, Vol. 88, No. 1, pp.78-83. <https://doi.org/10.1302/0301-620X.88B1.16446>.
- [37] Kleinlugtenbelt IV, Bakx PA & Huij J (2010), "Instrumented Bone Preserving elbow prosthesis in rheumatoid arthritis: 2-8 year follow-up", *J. Shoulder Elbow Surg.* vol. 19, pp. 923-928. <https://doi.org/10.1016/j.jse.2010.05.003>.
- [38] Gilot G, Alvarez-Pinzon AM, Wright TW, Krill M, Routman HD & Zuckerman JD (2015), "The Incidence of Radiographic Aseptic Loosening of the Humeral Component in Reverse Total Shoulder Arthroplasty", *J. Shoulder Elbow Surg.*, Vol. 24, pp.1555-1559. <https://doi.org/10.1016/j.jse.2015.02.007>.